Lehigh University

Annual Progress Report: 2010 Formula Grant

Reporting Period

January 1, 2011 – June 30, 2011

Formula Grant Overview

Lehigh University received $88,081 in formula funds for the grant award period January 1, 2011 through December 31, 2012. Accomplishments for the reporting period are described below.

<u>Research Project 1: Project Title and Purpose</u>

Effects of Cx43 Over-expression on Cell Proliferation and Skeletal Patterning During Fin Regeneration - Mutations in connexin genes lead to a variety of human diseases. In particular, mutations in human *CX43* cause skeletal malformations associated with oculodentodigital dysplasia. Remarkably, mutations in zebrafish *cx43* cause skeletal defects similar to those observed in human, revealing that the function of *cx43* is conserved. However, it remains unknown how connexin mutations cause defects in cellular functions leading to human disease. The purpose of this research is to identify changes in cell division and gene expression associated with overexpression of zebrafish *cx43*. Thus, results from this research project will provide insights into the underlying molecular mechanisms associated with changes in Cx43 activity. Revealing how connexin function regulates cellular function is the first step towards understanding how connexins mediate disease phenotypes.

Anticipated Duration of Project

1/1/2011 - 12/31/2012

Project Overview

Identification of the molecular mechanisms controlling size and shape represents one of the fundamental unanswered problems of biology. In particular, the vertebrate skeleton consists of bones of various morphologies whose size and shape are the result of precisely coordinated cellular activities, such as cell proliferation and gene expression. We utilize the zebrafish fin skeleton to provide insights into the underlying mechanisms regulating bone size and shape. The fin length mutant *short fin* (*sof* ^{b123}) has short fins due to defects in the length of the bony fin ray segments, and the *short fin* phenotype is caused by mutations in the gap junction gene *cx43*. Gap junctions permit the exchange of small molecules, such as ions and metabolites (i.e., not nucleic acids or proteins), between adjacent cells. Remarkably, mutations in human *CX43* cause oculodentodigital dysplasia (ODDD), a syndrome affecting the morphology of the human craniofacial and distal limb skeletons. Thus, the function of *cx43*, albeit unknown, is conserved during skeletal development. However, it remains unclear how defects in direct cell-cell

communication of this type regulates tangible cellular activities, such as cell proliferation and gene expression. The major goal of this project is to establish a transgenic line overexpressing *cx43* to reveal how increased Cx43 affects cell proliferation and joint formation. Thus, the aims are to evaluate changes in cell proliferation and skeletal differentiation at different levels of *cx43* overexpression. Cell proliferation will be evaluated using standard methods, such as bromo-deoxy-uridine (BrdU) labeling and detection of different stages of the cell cycle (i.e., interphase and mitosis). Cellular differentiation will be evaluated by following changes in gene expression for osteoblast-specific genes and for joint-forming cell-specific genes. Thus, the newly established transgenic line represents a critical tool for this project as well as for future hypothesis-driven aims that will be used to define the underlying mechanism of Cx43-based changes in cell proliferation and joint formation. Data resulting from this project will therefore provide important insights into how Cx43 function regulates the correct patterning of bones and joints.

Principal Investigator

Mary K. Iovine, PhD
Associate Professor
Lehigh University
111 Research Drive
Iacocca B217
Bethlehem, PA 18015

Other Participating Researchers

None

Expected Research Outcomes and Benefits

Oculodentodigital dysplasia (ODDD) is a human disease of the craniofacial and distal limb skeletons caused by mutations in the *CX43* gene. The underlying mechanism leading to the skeletal phenotypes of ODDD is unknown. Moreover, it remains largely unclear how defects in gap junctional communication lead to tangible changes in cellular function such as cell proliferation and gene expression. The research described in this project provides strategies to define the molecular and cellular changes induced by Cx43 activity during zebrafish fin regeneration. Indeed, Cx43 function during skeletal morphology is highly conserved, suggesting that insights provided by the zebrafish fin skeleton will be applicable to human disease phenotypes. Using the zebrafish fin skeleton, it is possible to readily monitor changes in the growth and differentiation of the cells contributing to the bony elements. Previous results have shown that Cx43 function is required for two important events during fin regeneration, cell proliferation and joint formation. Here, a newly generated *cx43* transgenic line will be utilized to define Cx43-dependent downstream changes leading to differences in cell proliferation and cell differentiation. Completion of this project will therefore provide insights into the requirements for Cx43 in the cells of the skeleton, and into the progression of ODDD.

Summary of Research Completed

The goals of this award are to first establish a new transgenic line in zebrafish that over-expresses the gap junction protein Cx43. Further goals are to reveal the effects of Cx43 over-expression on cell proliferation and cell differentiation during skeletal morphogenesis in the zebrafish fin. Since the award was made, we have identified three founders that each representing an independent transgenic line. Currently, we are validating that these lines are what we expect.

The founders were generated by injecting the transgene (*hsp70:cx43-egfp* flanked by the Tol2 transposon repeats) and the mRNA for Tol2 transposase into embryos. The *hsp70* promoter is the "*heat-shock 70*" promoter, and is activated in most cells by high temperature. Therefore, it is possible to inducibly and reversibly express the Cx43 protein fused to EGFP. Following injection at the one-two cell stage, the transgene is randomly inserted throughout the genome and in multiple cell types. Founders represent chimeric adults that carry the transgene in some cells, and may carry the transgene in their germ line. Individuals that carry the transgene in their germline are considered "transgenic" since the transgene will continue to be propagated by continued matings. Identification of the founders was attempted using two methods: genotyping by PCR and screening for EGFP expression.

In order to identify possible transgenic carriers (i.e., carriers of the transgene in the germline), we first completed PCR-based genotyping of fin DNA. The caudal fin is amputated and treated with proteinase K to release cell contents. The resulting cell lysate is treated with phenol:chloroform to dissolve the protein component. The remainder represents the template DNA to be used for genotyping. To identify founders, we completed PCR on fin-clipped DNA using primers that span the *hsp70* promoter and the *cx43* coding sequence, since these sequences are only in close proximity in the transgene. This strategy yielded five possible transgenic carriers (out of about 300 adults). To determine if any of these founders carried the transgene in their germline, each founder was outcrossed to wild-type (C32 strain). None of the progeny from these crosses yielded transgenic individuals.

A second method to identify founders involves screening for EGFP. Fortunately, it has been noticed that the *hsp70* promoter is "on" in the lens of the zebrafish under typical growth conditions (i.e., and does not require "heat shock"). Therefore, from 48 hours post fertilization (hpf) and onward, detection of EGFP fluorescence in the lens indicates the presence of the transgene in those cells. This is a facile method for detection of chimeric F0 founders when EGFP is expressed behind the *hsp70* promoter. This method has identified 15 possible founders out of 300 adults (i.e., none of these overlapped with those identified by genotyping). So far, we have outcrossed three of the 15 (all three were males). Remarkably, progeny from all three males include transgenic fish. The frequency of transgenic progeny is about 90 % from male 1, about 95 % from male 2, and about 50 % from male 3.

We are in the process of confirming that cells in the fins express the transgene, and that the Cx43-EGFP fusion protein is over-expressed. At 5 days post amputation (dpa) we expose transgenic fish to heat shock (i.e., 38°C) for one hour. Five hours later, fins are harvested in

fixative (i.e., to evaluate fins for immunofluorescence or gene expression) or processed for quantitative RT-PCR (qRT-PCR) or immunoblotting. These studies are underway.

Research Project 2: Project Title and Purpose

Modular Design of Hybrid Nanoparticle-Peptide Systems as Novel, Stimuli-Responsive Cancer Therapeutics - The purpose of this project is to design, synthesize and characterize a series of multifunctional, hybrid materials with unique, responsive physical and biological properties as drug delivery systems targeting cancer. Targeting cancer cells *in vivo* is a significant challenge due to the multifaceted nature of the process of metastasis, and therefore requires a sophisticated approach in which specificity and rate of drug release are tightly controlled. Nanoscale carriers offer an attractive method to deliver targeted therapies due to their ability to overcome in vivo transport limitations, traverse cell membranes and control rate of intracellular drug release. By integrating peptide-based tethers to control biological targeting *in vivo* with inorganic hybrid nanoparticles, we will have multiple, independent methods to control the targeting, uptake and release of drugs *in vivo*.

Anticipated Duration of Project

1/1/2011 - 12/31/2012

Project Overview

The *overarching research objective* of this project is to develop hybrid, pH-responsive nanoparticle carriers capable of targeted, controlled drug delivery to cancer cells that are robust to the dynamic nature of metastasis. Conventional drug delivery approaches have focused on organic particles as nanoscale carriers with engineered ligands to achieve specificity. While effective in some instances, these carriers suffer from chemical instability and immunogenicity, reducing the effective half-life *in vivo*. In addition, the lack of fine control over porosity of organic particles (i.e., wide distribution of pore sizes and surface characteristics) limits the resolution with which drug release kinetics can be controlled and ultimately tuned. One intriguing, yet less explored alternative is the use of appropriately functionalized inorganic nanoparticles that hold potential for addressing all of these concerns. The *underlying hypothesis of this project* is that pH-responsive, protease-susceptible peptides can be employed to tether clusters of (e.g., size, porosity) micro-, meso-, and/or hierarchically porous inorganic nanoparticle drug carriers as a means for achieving *in vivo* drug targeting and specificity, and for enhancing overall efficacy of cancer drug delivery. Specific project aims include:

1. Design of a family of pH-responsive peptides with engineered protease cleavage sites to act as particle 'tethers'
2. Synthesis of host micro-, meso-, and hierarchically porous inorganic (e.g., silica) nanoparticles with controllable functionality and pore characteristics (e.g., ordering, size, functionality) as robust drug carriers with tunable signatures for drug release
3. Assessment of how particle size, peptide tether-mediated interparticle cross linking, pore size, and pore surface characteristics influence residence time, affect entry into cancer cells, and control drug release

We plan to use a number of biophysical methods, including tryptophan fluorescence, circular dichroism and absorbance spectroscopy, to characterize the folding and assembly of our designed peptides as a function of pH, and electron microscopy, nitrogen adsorption, and x-ray scattering to characterize the structure, morphology, and textural (pore, surface area) properties of the inorganic nanoparticles. Flow cytometry, fluorescence confocal microscopy and enzyme-linked immunosorbent assay (ELISA) binding assays will be used to probe how specific features of the hybrid materials affect drug uptake and viability of cancer cells in culture.

Principal Investigator

Bryan W. Berger, PhD
Assistant Professor of Chemical Engineering
Lehigh University
B320 Iacocca Hall
111 Research Drive
Bethlehem, PA 18015

Other Participating Researchers

Mark A. Snyder, PhD – employed by Lehigh University

Expected Research Outcomes and Benefits

The *expected outcome* of this project is the identification of key features of hybrid organic-inorganic nanocarriers to control the rate of drug release. Beyond establishment of novel drug nanocarriers, a primary benefit of this project will be the development of a general knowledge base for rational design of more effective cancer therapeutic delivery mechanisms. Specifically, elucidation of the physical and chemical parameters governing drug release from inorganic particles (e.g., particle size, porosity, polydispersity, host-guest interactions) will prove essential for the rational design of hybrid carriers composed of tethered porous particles whose properties have been individually tailored to favor long- versus short-release rates of drug *in vivo*, and, as such, targeted and sustained drug release over short, intermediate, and long-time limits. Results from this project will further illustrate how peptide folding and structure contribute to the stability of the hybrid material *in vivo*, and how designing and controlling pH-sensitivity of peptide tethers will allow exposure of specific protease cleavage sites only in the vicinity of targeted cancer cells, a process critical to the release of inorganic particles as drug carriers. While peptides have been employed as epitopes or ligands to bind specific cell-surface receptors to achieve specificity, these mainly act as passive targeting mechanisms that lack responsive elements capable of *in vivo* differentiation of cancer and normal cells. By coupling multiple, folding-dependent mechanisms into the peptide structure, we expect this project to provide a more specific mechanism by which to target cancer cells. Furthermore, very little work has been done to investigate how integrated inorganic-organic materials function *in vivo* as drug carriers. Finally, this project will provide a detailed, quantitative analysis of the efficacy of inorganic-organic materials as nanocarriers that can serve as a template for future hybrid material design projects. Advances in cancer cell targeting *in vivo* are a major challenge, and are critical to

improving health status and outcomes associated with lung, liver and other forms of cancers due to tobacco use.

Summary of Research Completed

Materials and Methods:
Cell culture: HEK293T cells were purchased from ATCC, and growth media and other tissue culture reagents were purchased from VWR. Cells were grown in 12- or 96-well dishes in a CO_2 incubator (Shel Laboratories) under standard growth conditions (5% CO_2, 80% humidity). FITC-phalloidin, DAPI, Fluoromount and other staining reagents were purchased from Sigma. Flow cytometry (BD FACS Canto II) and epifluorescence microscopy (Nikon Eclipse) were available as part of the Lehigh University Biological Sciences core facility. The gene encoding for human legumain was purchased from OpenBiosystems, and subcloned into vector pEGFP-N1.

Peptide characterization: Peptides were purchased from the Penn State Hershey Medical Center Peptide Synthesis Core Facility and purity confirmed using MALDI (Bruker; Lehigh University Department of Chemistry core facility). Peptides were dissolved in buffers at appropriate pH values and concentration measured using UV-visible spectroscopy (GE Ultrospec Pro). Samples were analyzed using circular dichroism spectroscopy (Jasco; Lehigh University Department of Chemistry core facility) using 1 cm path length quartz cuvette at 20°C.

Particle synthesis: Reagents for particle synthesis, tetraethylorthosilicate (TEOS, 98%, Sigma-Aldrich) and L-lysine (Sigma-Aldrich), and fluorescent labeling (Rhodamine 6G; Sigma-Aldrich, dye content ~95%) were purchased and used as received. Optically clear solutions of silica nanoparticles were synthesized by addition of prescribed amounts of TEOS to aqueous solutions of L-lysine, to yield final molar compositions of x SiO_2/y L-lysine/9500 H_2O/4x ethanol, where x=10, 61.5, 61.5 and y=5.8, 1.23, 1.23, respectively, for the ca. 5 nm, ca. 10 nm, and ca. 20 nm particles. 5 nm particles were synthesized at room temperature under vigorous stirring (approximately 1000 rpm). The ca. 10 nm and 20 nm particles were synthesized at 60°C (24 hrs) and 90°C (48 hrs), respectively, under stirring at 500 rpm. Rhodamine 6G was incorporated into the particles by two approaches. In a direct incorporation approach, 0.5 mL of a 6 mM aqueous Rhodamine 6G solution was added to 20 mL aqueous L-lysine solution prior to the addition of TEOS. In an alternative approach employed for the ca. 10 nm particles, silica nanoparticles were first prepared according to the procedure above. To 33 mL of the resulting clear nanoparticle sol, 62 μL of 6 mM Rhodamine 6G solution was added and allowed to stir for approximately 5 minutes. 146 μL of TEOS was then added, and the solution was allowed to stir at 50°C for 12 hr. In both cases, unincorporated dye was purified from solution by centrifugation at 25,000 rpm for 60 min, decantation of the supernatant, and redispersion by sonication in purified water with a pH of 4.0 (pH adjusted with 0.25 M HCl). The purification process was repeated four to five times. Finally, the particles were redispersed in purified water via sonication for 60 min.

Particle characterization: Dynamic light scattering (DLS) was employed to characterize the size of synthesized silica particles. As-made samples were filtered with a 0.2 micron syringe filter into dust-free light scattering cells for analysis. The CONTIN method[R1] was subsequently employed to determine the hydrodynamic radius of the suspended particles. Complementary

transmission electron microscopy was carried out by drying a droplet of the nanoparticle sol on TEM grids, followed by imaging with a JEOL 2000. UV-visible absorption spectra of the fluorescently labeled nanoparticle sols were measured (GE Ultrospec Pro) against a blank water reference for verification and quantification of dye incorporation. Dye leaching studies were carried out over a period of 72 hours by measuring UV-visible absorption of the solvent (particle free) collected from the centrifuged nanoparticle sols (25,000 rpm for 60 min).

Results:

Particle sizing and verification of dye incorporation: Clear nanoparticle sols were produced containing approximately 1% v/v of silica nanoparticles. DLS measurements (Fig. 1) show that the particle populations are monodisperse and have been prepared with approximately sizes corresponding to the expected size. Representative TEM images of the ca. 10 nm and ca. 20 nm particles (Fig. 1) confirm this particle sizing, and highlight the high degree of monodispersity of the prepared particles. UV-visible spectra collected from the fluorescently labeled particles following removal of all unincorporated dye (Fig. 1) clearly show the successful fluorescent labeling of the particles. Due to preparation conditions and particle volume, the amount of incorporated dye increased with particle size, with approximately 1, 5, and 11 molecules of Rhodamine 6G per 5 nm, 10 nm, and 20 nm particles, respectively. Stability of the fluorescently labeled particles against leaching of the dye was deemed critical beyond the timescale of experiments conducted in this work in order to avoid non-specific fluorescent labeling of cell features. Studies, however, confirmed negligible leaching of the particle-incorporated dye.

Particle uptake into HEK293T cells: We used 2 complementary methods to investigate how particle size affects uptake and subcellular localization within HEK293T cells. First, we used an end-point assay in which cells were incubated with varying concentrations of rhodamine-labeled nanoparticles of varying size (5, 10 and 20 nm) for 48 h, then imaged to determine subcellular distribution. For all 3 particle sizes, we do not see evidence for enhanced cell toxicity in the presence of nanoparticles, as cells remained viable and proliferated over the 48 h experimental window similar to untreated cells. Interestingly, we see the greatest uptake at 5 nm, with nanoparticles broadly distributed throughout the cell cytoplasm, actin-rich filaments and subcellular organelles (Fig. 2). Several studies using silica-based nanoparticles have indicated nanoparticles preferentially accumulate in endocytotic vesicles, suggesting an activated transport mechanism. However, our results indicate the 5 nm particles are able to freely diffuse throughout the cell and do not adversely impact cell growth or proliferation. Thus, the silica-based nanoparticles exhibit high accessibility and low inherent toxicity, making them (or silica-shelled particles of the same size) ideal for our proposed hybrid organic-inorganic drug delivery system.

Second, we investigated the kinetics of particle uptake using flow cytometry. Particles were incubated with adherent or suspension cells in a 96-well dish and the extent of particle uptake determined using the change in forward- and side-scatter as well as rhodamine fluorescence. Due to the large size and density difference between nanoparticles and HEK293T cells, we can separate both populations using forward- and side-scatter, and correlate the rate of particle uptake through the increase in cell forward- and side-scatter as well as apparent rhodamine fluorescence. As illustrated in our FSC-SSC plot (Fig. 3), we can easily resolve treated from untreated cells with rhodamine-labeled nanoparticles, and therefore use the shift in rhodamine-positive cell population peak position as a measure of particle uptake. Interestingly, we observe a

clear optimum in uptake for the suspension cells in the presence of 5 nm particles, with rapid uptake over the course of 2 h, whereas adherent cells show a reduced rate of constant particle uptake over the 6 h window (Fig. 3). Larger particle sizes (10 nm) exhibit a slow, monotonic particle uptake rate independent of adherent or suspension cells. Thus, consistent with our initial imaging results, we observe the greatest rate of uptake for 5 nm particles in the presence of suspension cells.

Peptide folding and structure: Of our 3 initial peptide designs, 2 exhibited moderate solubility in pH 7 aqueous buffer (0.1-1 mg/mL) and the third was highly soluble (> 5 mg/mL). We characterized each of these peptides at pH 7 by circular dichroism (CD), and found that the 2 moderately soluble peptides both exhibited a sharp, pH-dependent transition between pH 5 and pH 6, as predicted based on our design. Each peptide contains a central asparagine flanked by alanine, which provides a consensus cleavage sequence for the legumain protease upregulated in metastatic tumors. Based on previous studies, the presence of an extended histidine-tryptophan network with 4-residue periodicity would be expected to provide a side-chain dependent stabilization of helical structure at low pH, whereas the deprotonated state at physiological pH should destabilize helical structure through direct interaction with the peptide amide backbone. Consistent with this prediction, one of our initial designs (R1; NH_2-EAHARAWANAHAEAWA-COOH) exhibits a strong, mixed α/β CD signal at low pH and a sharp transition between pH 5 and pH 6 to a predominantly β-sheet signal (Fig. 4). One interesting result is the lack of dominant helical structure at low pH despite the expected histidine side-chain dependent helical stabilization, with a spectrum that instead resembles a mixture of α-helix and β-sheet, whereas above pH 6, the spectrum shifts towards exclusively β-sheet rather than turn or random coil (Fig. 4). Our attempts to use CDPRO to quantify the secondary structure composition of the peptide at each pH were unsuccessful due to a poor fit between the experimental and predicted CD spectra, but the general trends we observe experimentally are also suggested by the preliminary CDPRO analysis. Thus, our designed peptides exhibit a strong, pH-dependent conformational change over the appropriate pH window (5-6), and the increase in α–helical structure at low pH should provide an increased rate of legumain cleavage relative to a β–sheet structure at physiological pH. Several studies of protease cleavage sites in proteins of known structure indicate that sites present in α-helical or loop structures are often cleaved *in vivo*, whereas predicted substrates present in β-sheet structures are typically inaccessible and therefore not cleaved.

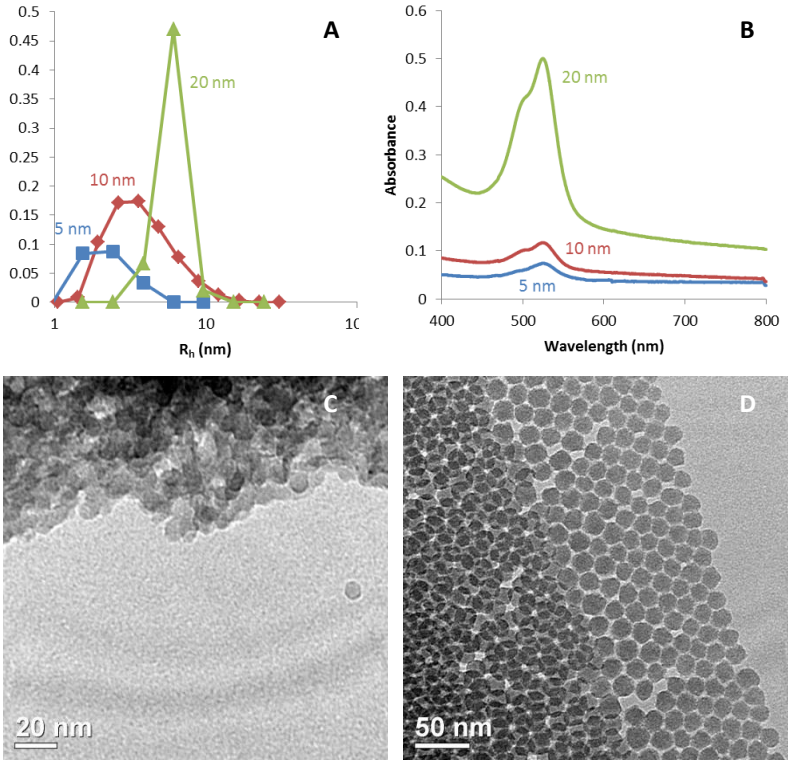

Figure 1: Nanoparticle characterization by (A) dynamic light scattering verifying particle stability and dispersion, with complementary TEM (C,D) images of dried ca. 10 and ca. 20 nm particle sols. UV-visible data for dye-labeled particles of all three characteristic sizes clearly confirms dye incorporation.

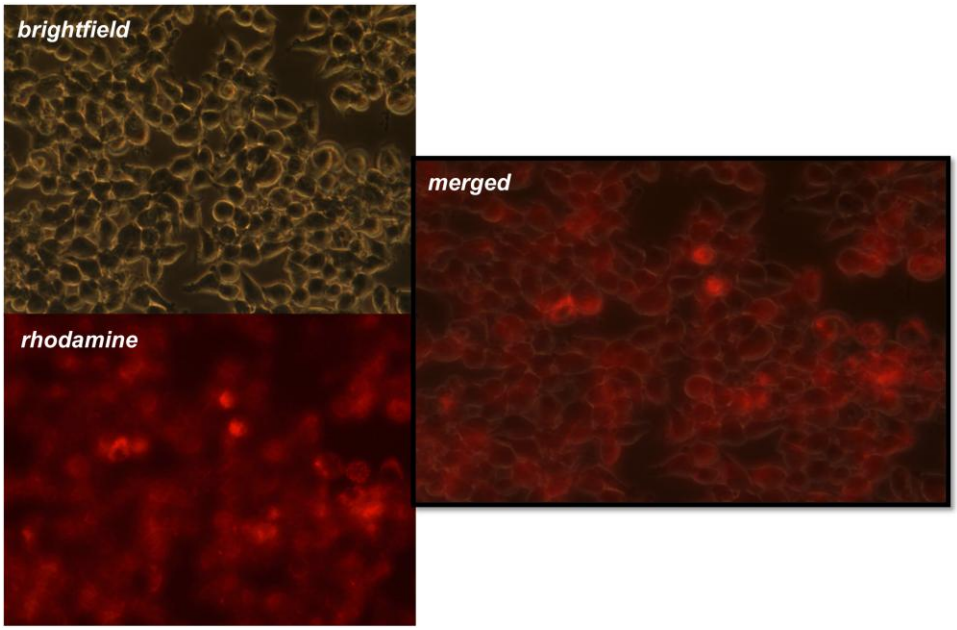

Figure 2: Epifluorescence imaging of particle uptake into HEK293T cells. Cells were treated with rhoadmine-labeled 5 nm particles for 48 h, washed to remove free particles and then imaged (20x objective) using epifluorescence microscopy. Note the dense cell growth visible by brightfield microscopy, indicative of robust growth and adherence in the presence of the nanoparticles, as well as the essentially complete overlap with rhodamine-positive regions imaged using epifluorescence. From the merged image, it is clear that the rhodamine particles are present throughout the cell cytoplasm, and the overall lack of punctate staining suggests the particles are not localized to a particular endosomal compartment or other internal organelle.

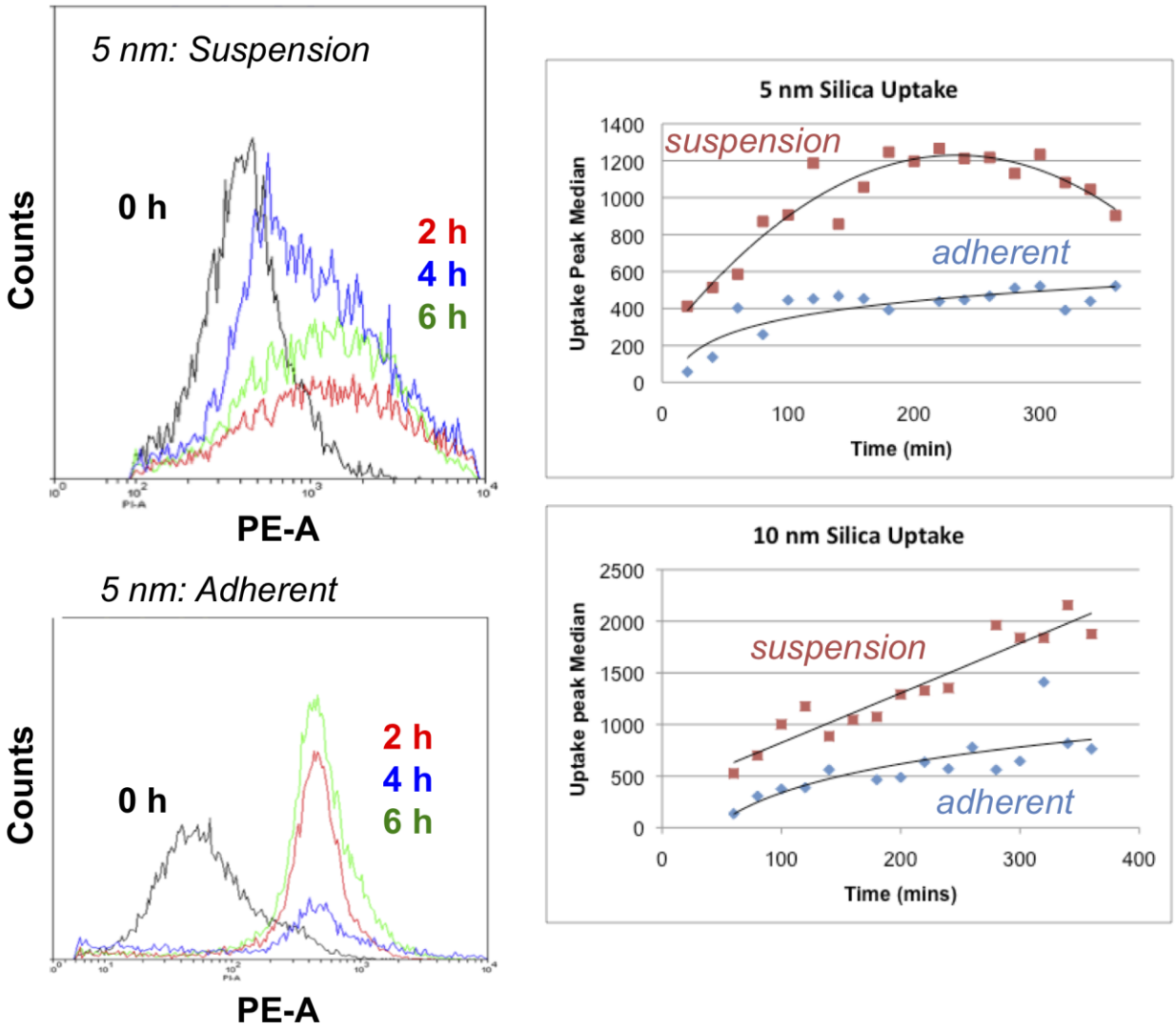

Figure 3: Particle uptake monitored by flow cytometry. Cells were treated with rhodamine-functionalized nanoparticles and the rate and extent of uptake monitored by the change in PE peak position with respect to time. Note the difference in peak width as well as position for adherent versus suspension cells. Peak position is plotted as a function of time for both 5 and 10 nm nanoparticles, comparing uptake rates for adherent versus suspension cells. Note the rapid rate of uptake and optimum in terms of 5 nm particle uptake for suspension cells relative adherent cells, which show a relatively slow rate of uptake. A similarly reduced uptake was observed for 10 nm particles as well, independent of whether they are suspension or adherent.

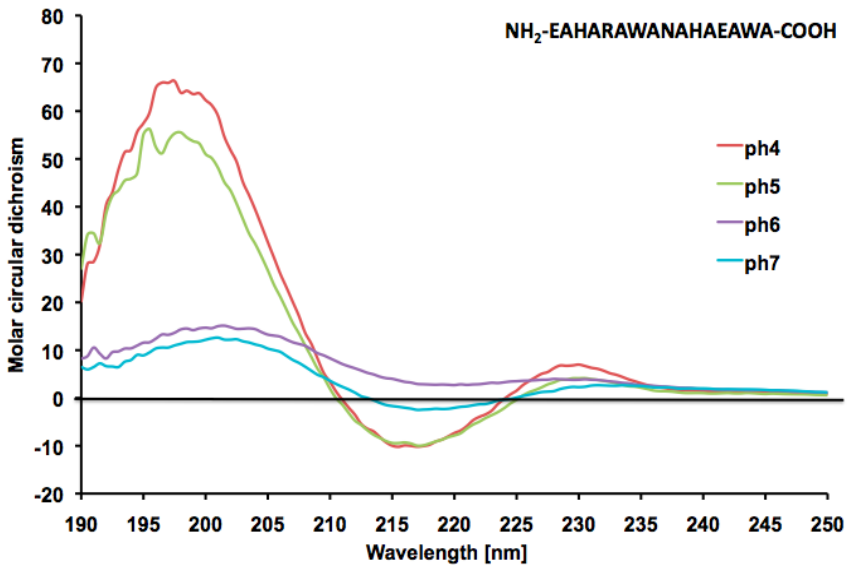

Figure 4: Circular dichroism analysis of peptide tether secondary structure as a function of pH. Peptide (0.1 mg/mL) was dissolved in buffer at various pH values and CD spectra measured using 1 mL samples in a 1 cm quartz cuvette at 20°C. Spectra were independent of concentration in the range of 0.05-1 mg/mL. A pH dependent transition from mixed helix/sheet below pH 5 to sheet above pH 6 was observed.

Research Project 3: Project Title and Purpose

Competition, Health Outcomes, and Resource Use in Hospitals - Public disclosure of data rating the performance of hospitals and physicians -- often referred to as report cards -- has proliferated in the 1990s, with the rationale that providing more information may increase hospitals' incentive to provide a higher quality of care, particularly when hospitals engage in quality competition. In this project we will examine the effect of Coronary Artery Bypass Graft (CABG) report cards on quality competition among hospitals in Pennsylvania. Our goal is to examine whether the availability of quality information intensified hospitals' quality competition, as revealed by individual patient outcomes, and to determine whether the strength of this effect varied with market concentration.

Anticipated Duration of Project

1/1/2011 - 12/31/2012

Project Overview

In this project we will study the relationship between better quality information, quality competition, and market concentration by examining how the online publication of CABG report cards affected health outcomes of individual Pennsylvanians living in hospital markets of differing degrees of concentration. We have three specific aims. *First*, we examine the impact of online publication of CABG report cards on quality competition among hospitals. *Second*, we

examine whether this impact is greater for patients that are more severely ill. *Third*, we examine whether this impact differs depending on whether patients are from rural or urban areas.

As in other studies of the effects of market concentration, potential endogeneity poses a major challenge for our analysis because unobserved heterogeneity may determine both the health outcomes as well as the extent of market competition. We address this problem using an approach recently developed by researchers examining the relationship between competition and quality, which is to measure market competitiveness based on predicted market shares. First, we estimate patient-level conditional logit models of hospital choice as a function of exogenous variables (e.g., marginal travel distance) that are not correlated with unobserved patient or hospital characteristics. We then calculate the predicted market share for each hospital using the estimates from the choice model. Finally, we calculate Herfindahl-Hirschman indices (HHI) based on these predicted patient flows (rather than actual patient flows), and assign them to patients based on their zip code of residence (rather than their actual hospital of admission). The competitiveness measures thus reflect the choices available to patients in their zip code of residence.

Our two main data sources are the inpatient data and the cardiac care report cards for CABG surgery providers collected by the Pennsylvania Health Care Cost Containment Council (PHC4). These two data sets allow us to examine the impact of the report cards on the quality of health outcomes realized by patients who have their procedure in hospitals located in markets with different degrees of competition. Using the health outcomes data available from PHC4 makes our research unusual and valuable exactly because it allows us to go beyond looking at costs and profits to examine the final results in health outcomes for Pennsylvanians.

Principal Investigator

Shin-Yi Chou, PhD
Professor of Economics
Lehigh University
Department of Economics
621 Taylor Street, Rauch Business Center
Bethlehem, PA 18015

Other Participating Researchers

Mary E. Deily, PhD – employed by Lehigh University

Expected Research Outcomes and Benefits

Two important policies implemented in Pennsylvania in the 1990s make this project significant. First, report cards were first published in Pennsylvania in the early 1990s as printed documents that were available at public sites such as libraries, or by request, making them relatively difficult to access. As of the second quarter of 1998, however, the reports have been posted on the PHC4 website (www.phc4.org), making them far more accessible. Second, in 1995 there were 37 hospitals in Pennsylvania that offered CABG because, as is the case in a number of states,

Pennsylvania restricted entry with a Certificate of Need (CON) program. There was, however, pressure from hospitals without CONs to enter this lucrative market, and in December 1996 the Pennsylvania legislature failed to extend the CON regulations restricting entry of new CABG programs. Within a few years more hospitals had opened their own CABG facilities, expanding the number of available suppliers to 58.

Thus, because of the expiration of the CON and the subsequent entry of new programs, many CABG patients in Pennsylvania faced hospital markets that experienced significant variation in concentration over time as well as across markets, while during the same period quality information about CABG programs became available online. In this project we will study the relationship between better quality information, quality competition, and market concentration by examining how the online publication of CABG report cards affected health outcomes of individual Pennsylvanians living in hospital markets of differing degrees of concentration.

If our results support our hypothesis that easier access to better information about health outcomes causes hospitals in more competitive markets to employ more resources to provide better health outcomes, it will provide strong support for continued publication of report cards and repeal of CON regulations. However, if these effects vary by patient severity or patient location (rural vs. urban), then these differential impacts must be incorporated in any evaluation of the effectiveness of these policies in improving patients' health outcomes.

Summary of Research Completed

Method

In this project we will study the relationship between better quality information, quality competition, and market concentration by examining how the online publication of CABG report cards affected health outcomes of individual Pennsylvanians living in hospital markets of differing degrees of concentration. Our very first step is to construct the market concentration measures.

We measure the market concentration using a version of the Herfindahl-Hirschman Index (HHI), the sum of squares of each provider's market share. A key concern in identifying the effects of market competition is its potential endogeneity to the outcome variables.

There are three commonly-used approaches to defining hospital markets: basing them on a hospital's service area, using a fixed geographic radius around the hospital, or using a variable radius around the hospital. While no single measure of a hospital's market is ideal, the service area approach is most problematic, since market boundaries are defined subjectively, while the variable-radius method, which defines the market radius that contains 75% or 90% of a hospital's actual patient flows, is considered to be superior for most research questions. Nonetheless, the variable-radius method has weaknesses.

First, the identification of the radius is determined by actual patient choices and thus the market definition will be affected by unobservable hospital characteristics such as quality. For example, a large teaching hospital may draw patients from a very wide area because of the breadth or high quality of its services. Market measures based on the area from which the hospitals patients were

drawn might suggest that the market was less concentrated that it actually is. A second, related, point is that the actual patient flows used to identify a hospital's market will in fact be an outcome of the competitive process. Third, such a measure only allows for a hospital to be entirely contained in, or excluded from, a given geographic market, which eliminates different degrees of substitutability among hospitals that may be perceived by patients due to variations in location. Finally, we are going to be interested in evaluating the impact of hospital competition on individual patients' health outcomes. Using the variable radius method to define hospital markets means that our measure of competition will be based on patient flows of the hospital where a patient was admitted, rather than reflecting the competition of the hospital market in which a patient lives. This approach may thus lead to correlation between competition and unobservable factors of a patient's health.

As a consequence, we construct our HHI measure of competition using predicted rather than actual market shares. The predicted market shares are based on conditional logit estimations of the probability of individual patients choosing individual hospitals within a 75 mile radius of their home zip code. We estimate patient-level hospital choice as a function of exogenous hospital and the patient's characteristics and the interactions between them. Relative distance (the extra distance an individual has to cover to go to the choice hospitals) enters a patient's utility function through interacting with the hospital's characteristics. The coefficients of the conditional choice model are then used to predict the hospital market share in each zip code area. Based on hospital's predicted demand coming from each zip code, we then aggregate the zip code-level predicted HHI to the hospital level. Finally, we measure HHI a patient faces using the weighted average of hospital-level HHI with the weights being the predicted hospital choices in patient's zip code of residence. HHI constructed in this method are less likely to be subject to the endogeneity with respect to hospital outcomes. Changes in predicted HHI originate from three sources: variations in the sizes of hospital markets through consolidation, entry, and exit, changes in patients' value trade-offs between travel distance to hospital preference, and changes in the distribution of patient populations.

Preliminary Data Analysis

Our principal data set, constructed and obtained from the Pennsylvania Health Care Cost Containment Commission (PHC4), is a record of all of the inpatient claims from Pennsylvania hospitals for the years 1995 to 2005. Distance measures were calculated based on zip code centroids of patients' residences and of hospitals' locations. We obtained some additional information about hospital characteristics, such as bed size, teaching status and technologies, from the American Hospital Association's Annual Survey of Hospitals. In the estimation of individual demand for hospitals, we include hospital report card grades for CABG surgery, which are also obtained from the PHC4. The report card information that is mostly recent to a patient's admission enters the demand equation as a quality characteristic of hospitals. We restrict our sample to Medicare patients who underwent a CABG procedure in the years 1995-2005: our preliminary sample consists of 92,428 patients.

Preliminary Findings

Table 1 reports the market structure of Pennsylvania CABG market. CABG hospitals were defined as hospitals submitting at least five claims for CABG during one year. The first two rows show that the number of CABG patients fell from 7608 in 1995 to 6316 in 2005, while the

number of hospitals performing CABG increased steadily, from 43 in 1995 to 61 in 2005. The most pronounced increase in the number of hospitals took place during 1996 to 1998, around the time when market entry barrier was reduced by the expiration of Certificate of Need (CON) regulation in Pennsylvania. Improved access to preventive care (such as beta-blockers and test for cholesterol level) has reduced the incidence of coronary artery disease and hence the need for CABG surgery. For those who need CABG, the introduction and diffusion of percutaneous coronary intervention (PCI) and stenting procedures has further reduced the demand for CABG. On the other hand, a hospital has incentive to offer cardiac surgical services because first, they are highly profitable under Medicare reimbursement schedule, and second, they improve the hospital's technology profile and thus attract more patients who might come to it for other services in the future. The rapid growth of HMO market share during 1990s may have increased such incentive because selective contracting managed care plans seem to value the presence of technology in making decisions about the network providers. As expected, the mean and median distance the patients travel to their admitting hospitals decreased over time, resulting from the improved access to CABG hospitals.

All these statistics seem to suggest that the Pennsylvania CABG market has become less concentrated over time. However, the submarket HHIs reveal somewhat different trends. The zip code-level HHIs predicted with or without hospital report-card information show that on average the zip code-level concentration fell slightly during 1995 to 2000 and then rose back afterward. One reason of this controversy may be that before 2000 providers in relatively remote areas (western and central PA) started to perform CABG surgeries, reducing the regional hospital concentration, while after 2000 most new entrants clustered in areas where the competition was already fierce (Southeastern PA), leaving the other regional markets more concentrated. Such trend is manifested in Figure 1. The fixed radius method yields much higher HHIs than the conditional logit HHIs, although it pictures a similar trend of concentration over our study period. The variable radius method yields much lower HHIs than the conditional logit HHIs, but still suggests a similar trend of concentration.

Table 1. Measure of Pennsylvania CABG Market Concentration for Medicare Beneficiaries during 1995-2004

	1995	1996	1997	1998	1999	2000	2001	2002	2003	2004
Number of hospitals	43	43	48	52	53	54	59	62	63	61
Number of patients	7608	7963	8079	7311	7473	7837	7573	7123	7135	6316
Mean distance to hospitals	13.083	13.373	13.353	13.146	13.035	12.808	12.488	12.116	12.027	12.333
	[11.800]	[12.092]	[12.078]	[12.064]	[12.104]	[12.067]	[11.763]	[11.458]	[11.452]	[11.895]
Median distance to hospital of admission	8.896	9.093	9.173	8.670	8.670	8.472	8.414	7.970	7.858	7.970
Predicted HHI										
50-mile radius	0.398	0.397	0.390	0.379	0.373	0.356	0.361	0.380	0.388	0.385
75-mile radius	0.365	0.367	0.352	0.331	0.334	0.316	0.322	0.342	0.350	0.348
100-mile radius	0.341	0.340	0.325	0.309	0.311	0.298	0.306	0.321	0.338	0.329
Fixed radius HHI										
50-mile radius	0.587	0.592	0.578	0.575	0.572	0.545	0.566	0.580	0.578	0.589
75-mile radius	0.579	0.580	0.568	0.567	0.567	0.538	0.555	0.570	0.569	0.578
100-mile radius	0.570	0.573	0.559	0.561	0.562	0.532	0.549	0.565	0.562	0.572
Variable radius HHI										
95% patient flow	0.228	0.226	0.224	0.231	0.201	0.214	0.216	0.220	0.230	0.235
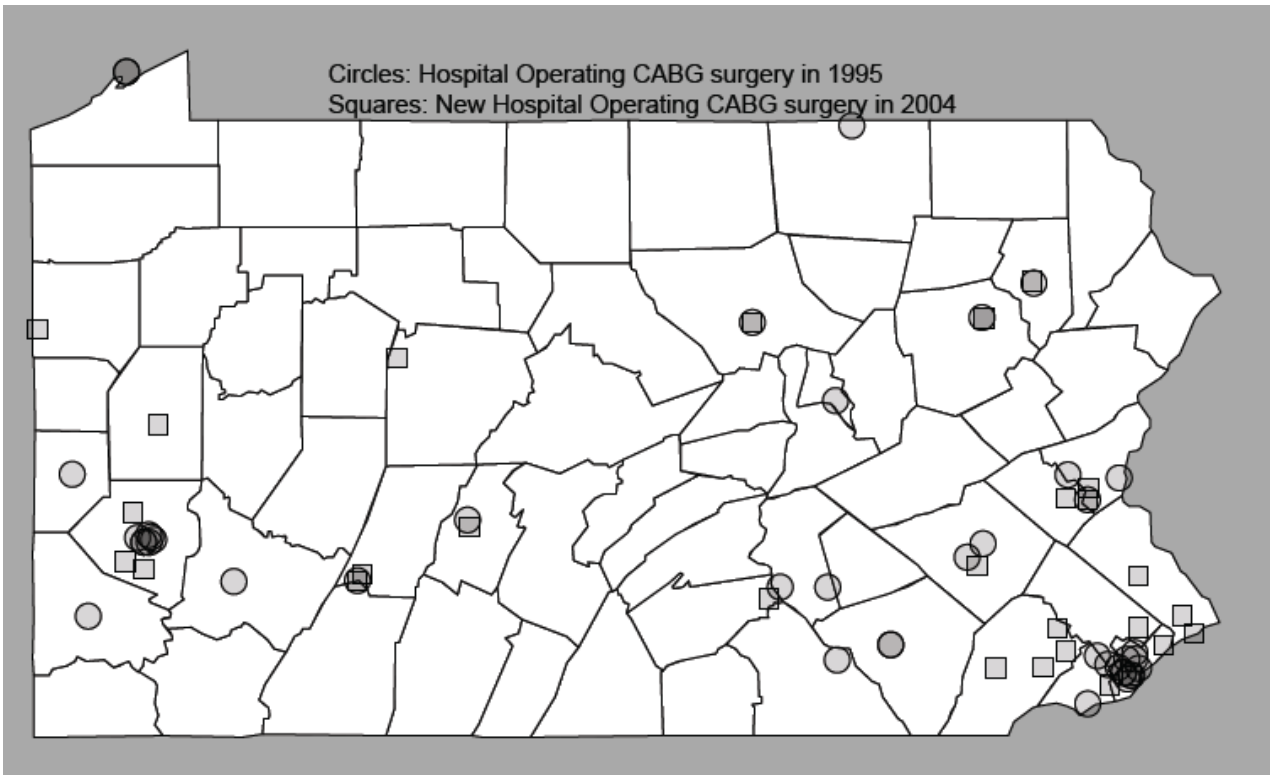
Figure 1. Geographic Illustration of Hospital Locations in Pennsylvania, 1995 and 2004